Collateral implications of carbon and metal pollution on carbon dioxide emission at land-water interface of the Ganga River

Kavita Verma

Ganga River Ecology Laboratory, Environmental Science Division, Centre of Advanced Study in Botany, Institute of Science, Banaras Hindu University, Varanasi-221005, India

Jitendra Pandey (jiten_pandey@rediffmail.com)

Banaras Hindu University

Research Article

Keywords: β-D-glucosidase, CO2 emission, Ganga River, Heavy metal, Land-water interface, Phenol oxidase

Posted Date: August 10th, 2021

DOI: https://doi.org/10.21203/rs.3.rs-759922/v1

Version of Record: A version of this preprint was published at Environmental Science and Pollution Research on November 25th, 2021. See the published version at https://doi.org/10.1007/s11356-021-17729-3.

Abstract

Atmospheric CO_2- source- and- sink is among the most debated issues that have puzzled climate change geochemist for decades. Here, we tested whether heavy metal pollutants in river sediments favor preservation of organic matter through shielding microbial degradation. We measured CO_2 emission and extracellular enzyme activities at land-water interface (LWI) of 7 sites along a 285 km main stem of the Ganga River and 60 locations up- and downstream of two contrasting point sources discharging urban (Assi drain; Asdr) and industrial (Ramnagar drain; Rmdr) wastewaters to the river. We found the lowest CO_2 flux at Rmdr mouth characterized by the highest concentrations of Cu, Cr, Zn, Pb, Ni, and Cd. The fluxes were relatively higher at locations up-and down-stream Rmdr. Substrate induced respiration (SIR), protease, FDAase and β-D-glucosidase all showed a similar trend but phenol oxidase and alkaline phosphatase showed opposite trend at the main river stem and Asdr. Sites rich in terrestrially derived organic matter have high phenol oxidase activity with low CO_2 emission. The CO_2 emission in the main river stem showed curvilinear relationships with total heavy metals ($\sum$THM; $R^2 = 0.68$; $P < 0.001$) and TOC ($R^2 = 0.65$; $p < 0.001$). The dynamic fit model of main stem data showed that the $\sum$THM above 337.4 μg g^{-1} were able to significantly decrease the activities of protease, FDAase and β-D-glucosidase. The study has implications for understanding C-cycling in human-impacted river sediments where metal pollution shields microbial degradation consequently carbon and nutrient release; and merits attention towards river management decisions.

Introduction

The loading of terrestrially-derived organic carbon (OC) influences ecosystem functioning in rivers and streams along hydrologic continuum, particularly through the processes controlled by microorganisms (Tezuka 1990; Taylor and Townsend 2010, Berggren and Giorgio 2015). Rivers and streams are the primary routes of delivering dissolved- and particulate organic carbon emerging from terrestrial landscapes through inland waters to coastal areas and oceans (Cole et al. 2007; Park et al. 2018; Siddiqui et al. 2020). Increased interest in understanding global carbon cycle, as it relates to climate change, has encouraged researchers to work on carbon capture, storage and release in rivers, oceanic and terrestrial systems (Jaiswal and Pandey 2019). Land-derived organic-C supply is an important energy source for riverine food webs and ecosystem functions, including carbon and nutrient cycling (Boyera et al. 2011; Pandey et al. 2014; Gessener et al. 2010; Rosemond et al. 2015). A large amount of terrestrially generated organic carbon enters into rivers and streams where it is decomposed accumulate in bed-sediment and transported downstream (Foulquier et al. 2015; Austin and Vivanco 2006). A substantial portion of terrestrial plant litter entering forested headwaters is processed immediately by heterotrophic microbes and invertebrate shredders, resulting in significant quantities of fine particulate organic matter which is transported downstream (Vannote et al. 1980). Furthermore, point sources releasing sewage and industrial effluents and non-point sources such as surface runoff are continuing to add massive amount of carbon and nutrients to streams and rivers (Bernot et al. 2010; Yadav and Pandey 2017). The presence of both the C-sources (allochthonous and autochthonous) allows uncoupling of primary- and secondary C-production and has implications for food web dynamics, CO_2 emission and riverine transport (Van den Meersche et al. 2009; Lau et al. 2009).

Being a conducive habitat for microbial metabolism, inland waters act as effective bioreactors, where terrestrial organic matter is rapidly decomposed (Richey et al. 2002). The organic matter is relatively short-lived in inland waters (mean residence time 2.5 ± 4.7 years), as compared to centennial to millennial-scale residence times in soils and oceans (Catalán et al. 2016). Because of multiplicity of factors that regulate organic matter turnover, such as C-chemistry, sediment characteristics, microbial composition, hydrologic control and disturbance, forecasting long-term stability of carbon compounds in large rivers is difficult (Kandeler et al. 1999; Dai et al. 2002; Schimel and Weintraub 2003). The microorganisms regulate biogeochemical transformations including the release of carbon dioxide (CO_2) (Guerin et al. 2006; Cole et al. 2007). Microbial degradation of organic matter in oxic sediments produces mainly CO_2. Because most of the inland waters are saturated with C gases, they constitute a net source of CO_2 to the atmosphere and are quantitatively important in ecosystem carbon budgets (Butman and Raymond 2011; Aufdenkampe et al. 2011; Teodoru et al. 2015). Despite these facts, the C-metabolism and CO_2 emissions of large rivers remain poorly quantified. Surface waters receive about ~1.9 Pg of carbon annually from different natural and

anthropogenic sources. About 0.2 Pg of this carbon undergoes burial in sediments and about 0.9 Pg is flushed to the ocean. The balance amount (0.8 Pg) returns to the atmosphere (Cole et al. 2007). Global emission of carbon dioxide from lotic waters is about 1.8 ± 0.25 Gt CO_2-C yr^{-1} (Raymond et al. 2013). This amount is equivalent to about 70% of the oceanic C sink globally (Le Quéré et al. 2014). According to Cole and Caraco (2001), the world's 80 largest rivers add about 0.15–0.3 Pg CO_2-C annually, whereas the inundated floodplains in humid tropics emit ≈ 0.9 Pg CO_2-C annually. This amount is about 3 folds of global riverine emission (Richey et al. 2002). The US Rivers and streams release about 2370 ± 800 g CO_2-C m^{-2} yr^{-1}(Butman and Raymond 2011). Because of strong hydrologic control and heterogeneity of sub-habitats, quantification and prognostics modeling of CO_2 emission in large rivers is very difficult (Jaiswal and Pandey 2019).

Our recent, multi-spatio-temporal scale studies show that, being a stable and biologically active zone, the land-water interface (LWI) of large rivers provides an imprint of hydrodynamic retention characterizing the processes and patterns in close correspondence with those occurring in the main river channel (Jaiswal and Pandey 2019). The LWI can be used as a stable testbed and predictor of river ecosystem responses to human disturbances (Jaiswal and Pandey 2019). The β-D-glucosidase, protease and FDAase are widely used to address soil/sediment microbial processes. The β-D-glucosidase catalyzes the terminal step in cellulose breakdown with subsequent release of glucose monomers to the microorganism (Dick 2011). The activity of this enzyme varies with soil/sediment types and positively correlates organic matter supply (Sinsabaugh et al. 2008; Yan et al. 2010; Mariscal-Sancho et al. 2010). Understanding the variations in β-D-gucosidase activity can help understanding sediment/soil C-metabolism and C-cycling (Jaiswal and Pandey 2019). The fluorescein diacetate hydrolytic assay (FDAase) is a widely accepted measure of total microbial activity in soils (Schnürer and Rosswall 1982; Battin 1997; Adam and Duncan 2001). The flourescien diacetate hydrolysis requires three major group of enzymes, esterases, proteases and lipases involved in the microbial decomposition of organic matter (Schnürer and Rosswall 1982). Also, it is used as a potential indicator of esterase activity of stream biofilms (Battin 1997). Phenol oxidase enters the environment through excretion or lysis and mediates lignin degradation and carbon mineralization (Sinsabaugh 2010).

Quantifying CO_2 emission and carbon sequestration in large rivers requires an understanding of factors that regulate microbial processes-linked C-metabolism. The processes which inhibit microbial activities reduce CO_2 emission. Metals, for instance, inhibit microbial activity (Ford 2000; Verma and Pandey 2019) and consequently, the CO_2 release (Dobler et al. 2000). Because most of the human impacted rivers simultaneously receive carbon and metal pollutants, it is expected that C enrichment will enhance CO_2 emission whereas metal pollutants will cause a stabilizing effect. Thus, countervailing effect of such disturbances is likely to create a complex pattern of C-dynamics challenging to predict CO_2 release/C-sequestration (Jaiswal and Pandey 2019). A clear understanding of such countervailing effects leading to unanticipated ecosystem consequences is essential for policy decision in river management. The purpose of this work is to fill the gap in our understanding of how point- and non-point sources of carbon and metal input affect C-metabolism and carbon dioxide emission at the LWI of the Ganga River. Here, we have attempted to establish mechanistic links between carbon and metal pollutants to develop a new context to understand collateral implications of human-driven stressors. The study was designed in two parts: First, to evaluate the effects of two contrasting point sources, one releasing metal-rich and the other releasing carbon-rich wastewater, on microbial extracellular enzyme activities and CO_2 emission at LWI; and second, to assess the collateral impacts and linkages with regulatory determinants at selected sites along the main stem of the Ganga River. We attempted to identify patches with variabilities and mechanistic regulatory control which can be used to quantitatively extrapolate system level CO_2 emission scenario for large rivers. The study has relevance in up-scaling system-specific scenario for improving prognostic models of CO_2 emission in addition to evaluating collateral implications of carbon and metal pollution in human-impacted large rivers.

Material And Methods

Study area

A two-year study (2017 to 2018) was conducted between Allahabad (25°28´N; 81°54´E) and Varanasi (25°19´N; 83°1´E) covering 285 km of the Ganga River. The sampling was done during low flow at six sites- Hatwa (Htwa), Sangam (Sngm), Sitamarhi (Stmh), Adalpura (Adpr), Ramna (Rmna) and Rajghat (Rjht). We consider the least-polluted site, Devprayag (Dvpg), ~ 812 km upstream to Hatwa, as a reference site. Also, we selected two contrasting point sources in Varanasi region (Assi drain, which discharge 66.4 mld urban sewage and Ramnagar drain, which discharge 24 mld of metal-rich industrial effluents) for trajectory analysis. For trajectories, we collected samples from 30 locations (each 100 m apart), selecting 15 up-streams and 15 down-stream of each point source (Fig. 1). The Ganga basin, a mixed landscape with predominance of highly fertile agricultural plains (>73% of the total area), support over 26% of India's population. The river experiences strong pressure from urban-industrial–agricultural releases and water regulation. The climate is tropical where March to June extends as a hot summer, July to October as a humid rainy season and November to February as a cold winter. About 90% of the annual precipitation (870-1130 mm) occurs in the rainy season. The relative humidity ranged from 27 to 83% (summer) and 58 and 99% (rainy). Summer temperature maxima may reach 46°C.

Sampling and analysis

Triplicate samples were collected from land- water- interface (LWI) of three sub-sites considered for each study site using sediment corers. Samples brought to the laboratory and preserved (4°C) for the analysis of microbial variables. Samples were dried at room temperature, homogenized, and sieved (2-mm mesh) for heavy metals .After digestion in a tri-acid mixture at a ratio of 5:1:1 (HNO_3/HCl/$HClO_4$) in a microwave digestion system (SINEO model MDS-6G), the samples were analyzed in a Perkin Elmer atomic absorption spectrophotometer (Analyst 800, USA). The detection limits were 0.0008 (Cd), 0.003 (Cr), 0.001 (Cu), 0.006 (Ni), 0.015 (Pb) and 0.001 (Zn) mg/l. The standard stock solutions and drift blanks purchased from Sisco Reaesrch Laboratories (India) were used to calibrate the AAS for respective metal. For spiking of samples, we prepare the solutions using nitrate salts of Cd, Cr, Ni and Pb and granules of Zn and Cu (99% purity). To ensure recovery strength, we repeatedly tested ratios of tri-acids and a 5:1:1 ratio showed ~99% recovery.

The sediment samples were analysed for granulometric fractions (Stemmer et al. 1998). Chlorophyll **a,** extracted in acetone, was determined spectrophotometrically (Lorenzen and Jeffrey 1980). Conductivity was measured using multiparameter tester (Oakton 35425-10, USA). The ammonium molybdate stannous chloride method was used to measure soluble reactive phosphorus (SRP; Murphy and Riley 1962). Total organic carbon (TOC) was quantified using a TOC analyzer (LOTIX TOC analyzer). Total nitrogen (TN) was analysed using Kjeldahl analysis and water soluble organic carbon (WSOC) following by Ciavatta et al. (1991).

Following a chloroform fumigation extraction, microbial biomass C (C_{mic}), was measured as per Jenkinson and Powlson (1976), biomass-phosphorus (P_{mic}) following Brookes et al., (1982) and nitrogen (N_{mic}) following Shen et al. (1984). The substrate-induced respiration (SIR) was assessed following Wardle et al. (1993). The microbial metabolic quotient was calculated in terms of BR/SIR ratio. Protease activity was measured in terms of aromatic acid released during casein proteolysis and expressed as L-tyrosine equivalents (Ladd and Buttler. 1972). Phenol oxidase was determined as described by Sinsabaugh and Findlay (1995) and alkaline phosphatase (AP) by Tabatabai and Bremner (1969). The β-D-glucosidase was assayed following Eivazi and Tabatabai (1988). For fluorescein diacetate hydrolytic assay (FDAase), the sample filtrates were incubated with fluorescein diacetate, and the fluorescein formed was estimated spectrophotometrically (Schnurer and Rosswall 1982).

The CO_2 at LWI was collected in steel chambers (23 cm height; 22 cm diameter). The chambers contain a small fan for distribution of air, and a thermometer to record temperature. The chambers were fixed 5 cm deep to ensure a seal against ambient air and the gas was withdrawn through a rubber fitted valve. For quality control, and to avoid changes in temperature and moisture regime, attempts were made to collect samples at an identical time. A polypropylene syringe with three-way stopper was used for withdrawing the gas from the headspace at 1-h interval. Samples were brought in an icebox and analyzed in a Trace 1110 Thermo Fisher Analyzer. The accuracy was validated by repeated calibration with standard gas samples.

Statistical analysis

Mean values of measurements are presented with standard errors (SE). Correlation coefficients and dynamic fit models were used to measure the extent to which variables covary. Principal component analysis was considered to verify major determinants. Confidence limit > 95 justifies significance. The Sigma plot (version 11.0) and SPSS (IBM SPSS statistics 20) was used for the statistical analysis. To find Euclidean distance and extent of dissimilarities, we used non-metric multidimensional scaling (NMDS) and Bray-Curtis neighbor-joining metrices.

Results

Main stem trends

CO_2 emission

The CO_2 flux at land-water interface varied between 83.9 mg m^{-2} h^{-1} (Rjht Site) and 339.2 mg m^{-2} h^{-1} (Sngm Site). The emission flux increased over time except at Rjht where it declined marginally on a temporal scale. At Sngm, the CO_2 emission was 4 folds higher than those at Rjht Site (Fig. 2).

Regulatory variables

Substrate-induced respiration (SIR) showed a trend similar to CO_2 emission. The enzyme activity-β-D-glucosidase, protease and FDAase did show maxima at Sngm Site and minima at Rjht Site whereas the microbial metabolic quotient (qCO_2) showed an opposite trend (Fig. 2). The phenol oxidase and alkaline phosphatase showed highest activity at Stmh Site and lowest at Rjht (Fig. 2).

Sediment characteristics

The concentration of metals in the riverbed sediment ranged from 42.2 to 161 μg g^{-1} (Zn), 35.2 to 188.2 μg g^{-1} (Cr), 10.2 to 170.2 μg g^{-1} (Cu), 10.5 to 82.4 μg g^{-1} (Pb), 0.5 to 7.8 μg g^{-1} (Cd) and 5.3 to 60.2 μg g^{-1} (Ni). The values were highest at Rjht followed by Sngm and lowest at Dvpg. The concentrations were highest for Cr and lowest for Cd (Fig 2). In the main river stem, the concentrations of total organic carbon (TOC), water soluble organic carbon (WSOC) and total nitrogen (TN) were high at downstream sites. At Rjht Site, the concentrations of TOC, WSOC and TN were 6 folds, 2.4 folds and 4.9 folds higher compared to their respective values at reference site Dvpg. The C:N ratio also was highest at Rjht Site. Microbial biomass carbon (C_{mic}), nitrogen (N_{mic}) and phosphorus (P_{mic}) and Chl **a** biomass showed trends similar to CO_2 emission, with values being highest at Sngm and Lowest at Rjht Site. Conductivity and SRP (soluble reactive phosphorus) also followed trends similar to TOC. The proportion of coarse sand was relatively higher at upstream site (Dvpg) and percentage of fine sand was highest at Adpr while clay was highest at Rjht (Table 1). The CO_2 emission showed curvelinear relationships with $\sum$THM (R^2= 0.68; P <0.001), TOC (R^2= 0.65; P <0.001) and phenol oxidase (R^2= 0.72; P <0.001) and significant positive correlations with FDAase, protease and β-D-glucosidase (R^2= 0.89 – 0.92; P <0.001) (Fig. 4).

Point source up-and down-stream trends

CO_2 emission

The CO_2 emission showed longitudinally variable trends at both the point sources. The CO_2 emission was found highest at the mouth of the Assi drain (Asdr; 432 mg m^{-2} h^{-1}) and decreased towards downstream and upstream sites. At the mouth of the Ramnagar drain (Rmdr), the CO_2 emission did show the lowest value (10 mg m^{-2} h^{-1}). At Rmdr, the CO_2 emission maxima at upstream sites of the drain was found 25 folds higher as compared to the mouth of the drain, whereas downstream maxima was over 38 folds higher. The CO_2 emission showed a gradual increase with distance upstream and downstream from mouth of the drain. The CO_2 efflux showed a wide variability and increased over time at Asdr but declined at Rmdr (Fig. 5).

Regulatory variables

At Asdr, the microbial/enzyme activities (SIR, FDAase, β-D-glucosidase and protease) all followed a trend similar to CO_2 emission with values being highest at the drain mouth. Metabolic quotient, phenol oxidase and alkaline phosphatase showed opposite trends (Fig. 5). Whereas at Rmdr, microbial/ enzyme (SIR, FDAase, β-D-glucosidase, protease, alkaline phosphatase and phenol oxidase) followed a trend similar to CO_2 emission with values being lowest at the drain mouth and increased towards downstream. Metabolic quotient showed an opposite trend (Fig. 5).

Sediment characteristics

The concentration of metals at Asdr ranged as: Cd, 2.3 to 15.2 μg g^{-1}; Cr, 36.2 to 118.3 μg g^{-1}; Cu, 22 to 51.2 μg g^{-1}; Ni, 21.3 to 78.2 μg g^{-1}; Pb, 42 to 77 μg g^{-1}; and Zn, 51 to 203 μg g^{-1}. At Rmdr, the values ranged as: Cd, 12.2 to 38 μg g^{-1}; Cr, 58 to 162 μg g^{-1}; Cu, 43 to 122 μg g^{-1}; Ni, 64 to 152.3 μg g^{-1}; Pb, 62 to 142 μg g^{-1}; and Zn, 51 to 250 μg g^{-1}. The concentrations were highest at drain mouth and values decreased towards upstream and downstream sites. Metal concentrations were 1.5 - 2.34 folds higher at Rmdr compared to Asdr (Fig. 6). The concentrations of WSOC, TOC, and TN, on spatio-temporal scale, showed similar trend at both the study drains. Asdr Site contained 1.5 folds high value of TOC and 1.2 folds high value of WSOC at the mouth as compared to Rmdr mouth. We found an opposite trend for total nitrogen. Microbial biomass-carbon (C_{mic}), nitrogen (N_{mic}), phosphorus (P_{mic}) and Chl **a** biomass showed trends similar to the CO_2 emission at Asdr with maxima at drain mouth (Table 2). We found lowest levels of microbial biomass and Chl **a** at Rmdr (Table 2, 3). The C:N ratio was found to be the highest at Rmdr mouth and lowest at Asdr mouth. Conductivity and SRP both were highest at Asdr mouth. Both the drains showed high percentage of clay at the mouth (Table 2, 3).

Principal component analysis

Principal component analysis (PCA) showed three significant PCs for the mainstem and Asdr, and two significant PCs for Rmdr (Table 4). For the mainstem, three PCs collectively explained 92.09 % of the variance. The first PC, which explains 62.12% of the variance, showed strong loading of heavy metals, qCO_2, TOC, TN, WSOC and sediment granulometry. Second PC explained 20.02% of the variance with strong loading of microbial activities, Chl **a** biomass and CO_2 emission. Third PC have strong loading of alkaline phosphatase and phenol oxidase with 9.95% variance. The first PC at Asdr (66.12% variance) showed strong loading of microbial activities, TOC, nutrient and granulometry while the second PC with 22.21% of variance showed strong loading of metals and qCO_2. The third PC (8.9% variance) separates phenol oxidase and alkaline phosphatase. For Rmdr, two significant PCs were obtained. The first PC explained 67.13% of the variance with strong loading of metals, TOC, TN, C:N ratio, silt, clay and qCO_2, whereas PC 2 explained 27.04 % of the variance and separates microbial activities and silt/clay (Table 4).

Discussion

Aquatic ecosystems serve as reservoirs of terrestrial and anthropogenic-C accumulation. Carbon enrichment interacts with site-specific conditions, including occurrence of other contaminants. Thus, the rate of decomposition vis-à-vis CO_2 emission varies subject to the nature of C-source and site-specific conditions, for instance presence of other contaminants. Anthropogenic input of carbon is often accompanied by a large supply of nutrient and non-nutrient contaminants (Smith and Schindler 2009). Thus, the fate of carbon in such water bodies can be strongly influenced by the interaction of multiple pollutants. For instance, nutrient supply, chiefly N and P, can gear-up autochthonous C- build-up and decomposition, whereas metal enrichment can provide countervailing effect. Thus, the complex interactions, especially those pertaining to countervailing effect deserve scaled-up studies from a climate change perspective; and for understanding ecosystem level effects of heavy metal pollution. Land-water interface (LWI) of large rivers provides heterogeneous habitats with imprints of riverine metabolism (Jaiswal and Pandey 2019). Here, we consider LWI to study C-metabolism and CO_2 emission as regulated by C- enrichment and metal-driven countervailing effects. This has concern because sewage sources alone add 110 Gg of TOC, 13.28 Gg DIN and 5.29 Gg of DRP annually into the Ganga River. In addition, the basin receives about 1.81 Tg, 2.77 Tg and 0.13 Tg of TOC, TIN, and P, respectively, through atmospheric deposition annually (Singh and Pandey 2018).

The CO_2 emission reported here was significantly lower than those reported for a freshwater marsh (1456.60 ± 593.31 mg m^{-2} hr^{-1}) and a brackish water marsh (1435.23 ± 689.71 mg m^{-2} hr^{-1}) in the Min River estuary, Southeastern China (Hu et al. 2017). Sediment with favorable conditions tends to be substrate limited, and show high *in situ* activities and low organic matter accumulation. In contrast, sediments with stress conditions, are activity limited, and show low *in situ* activities, promoting carbon storage (Sinsabaugh 2010). Also, the enzyme activity limited systems contribute to organic matter accumulation (Freeman et al. 2001; 2004). Earlier research shows that carbon quality and particle size distribution is an important regulator of microbial biomass distribution (Sinsabaugh and Findlay 1995). Small particle size support high concentration of TOC and TN, with concentrations generally high in clay, although the C:N ratio declines with diminishing particle size (Stemmer et al. 1998). The downstream sites- Sngm and Asdr, are rich in WSOC, TOC and TN concentrations and also have high percentage of clay and silt at mouth of the drain. High substrate availability coupled with high percentage of silt and clay may invite the colonization of a large microbial population and create a suitable room for high microbial/enzyme activities that trigger CO_2 emission.

Here we identified, in addition to other variables, two major determinants-chemical recalcitrance and heavy metal enrichment, to address changes in microbial extracellular enzyme (EE) activities vis-à-vis CO_2 emission along the river gradient. Microbial EEs mediate decomposition and mineralization of organic matter (OM), and terrestrially-derived OM often shows recalcitrance to degradation (Sinsabaugh 2010; Ward et al. 2013). Terrestrially derived OM, rich in leaf litter, are generally poor in N content (high C:N ratio) and are poorly decomposable relative to autochthonous C. Lignin and cellulose constitutes the most abundant C fractions on land (Boerjan et al. 2003). Lignin accounts about 30% of organic-C in the terrestrial C reservoir (Boerjan et al. 2003), and ~55% of land sequestered lignin is degraded in the river continuum (Malhi et al. 2008; Bose et al. 2009; Houghton et al. 2001). Roughly 80 Tg C in the Amazon terrestrial biosphere is fixed as lignin each year (Mayorga et al. 2005; Ward et al. 2013). Sites with chemical recalcitrance-measured in terms of phenol/phenol oxidase activity-a signature of terrestrially-derived OC; and those rich in metal pollutants showed mismatch in CO_2 emission rates and C-inputs. Phenol oxidase is one of the key enzymes able to degrade recalcitrant phenolic materials such as lignin (McLatchey and Reddy 1998). Phenolic materials are highly inhibitory to enzymes and their lower abundance at some sites allowed higher hydrolase activities. Sites- Stmh and Adpr, with high amount of terrestrially derived organic matter showed highest phenol concentration and high C:N ratio and CO_2 emission rates were not comparable to C inputs. The downstream sites- Sngm and Rjht, with easily utilizable soft carbon, added from sewage for instance, showed less activity of phenol oxidase, but high activity of β-D-glucosidase. Sites with high concentration of Chl **a**, (high autochthonous organic C) did show low phenol oxidase activity and high activity of β-D-glucosidase. The C:N ratio, a proxy of decomposability (Datry et al. 2018), was recorded lowest at highly productive site (Sngm). At the mouth of both the point sources (Asdr; Rmdr), the phenol oxidase activity was found to be the lowest which increased with upstream and downstream trajectories. Pandey and Yadav 2017 reported very low levels of DO close to the mouth of Assi drain. Thus, low amount of land-derived OC coupled with oxygen deficiency could decrease phenol oxidase activity, whereas the activity of hydrolases remained relatively higher even in an anaerobic environment (Lee et al. 1999). We also tested alkaline phosphatase (AP), an ectoenzyme of microbial origin, used as a measure of P status in soil and sediment (Sayler et al. 1979; Johnson et al. 1998; Sinsabaugh et al. 2009). The AP showed a trend similar to phenol oxidase, whereas sediment-SRP showed an opposite trend in the main stem as well as along point sources. Also, the sites with low productivity have high AP and phenol oxidase activities. Overall, these two enzymes can be used as an indicator of less polluted and low CO_2 emission sites; whereas, high activities of other enzymes indicate sites acting as a hot spot of CO_2 emission.

We further tested, whether heavy metal enrichment was able to reduce EEs activities and CO_2 emission in the main stem and source orientated sites. The countervailing effect of heavy metals at Rjht and Rmdr reduced CO_2 emission. The NMDS separated microbial biomass, EE activity, Chl **a** biomass and CO_2 emission in one group between the Sngm and Rmna (Fig. 7). Asdr also showed the similar pattern (Fig. 8), whereas Rmdr the NMDS showed that the microbial activity maximum at the downstream sites (Fig. 9).The granulometry and organic matter content affect the distribution of heavy metal (Farkas et al. 2009). Fine grained sediments tend to have relatively higher metal contents due in part to high specific surface of particles (Rubio et al. 2000). Positive correlations among metals, organic substrate and sediment particle size validate this concept. A

higher proportion of fine sized particles lead easy transportation of the sediment downstream (Bartoli et al. 2012). Accordingly, the river sites down the industrial- and the urban areas were significantly more polluted than upstream sites. The Rjht and Rmdr Sites showed carbon storage in bed sediment. Despite high substrate availability, there were relatively lower *in situ* microbial/enzymetic activities. Many investigators have reported that heavy metal stressors can induce change in the microbial biomass and activity (Khas et al. 1998; Jaiswal and Pandey 2018). The microorganisms release extracellular enzymes (EEs) to activate the lysis of organic matter (Romaní et al. 2004). The EEs are produced as a result of cellular metabolism influenced by carbon and nutrient availability. The EEs are highly sensitive towards toxicants, including heavy metals, and respond sharply to even after small changes in sediment quality (Pandey and Yadav 2017; Jaiswal and Pandey 2018; Verma and Pandey 2019). The Rjht Site at the main river stem and the sites located downstream of Rmdr showed high concentrations of total heavy metals, nutrients, TOC and high C:N ratios. Despite high TOC, an important resource/ substrate for microbial activity, reduced microbial biomass and enzyme activity at these sites indicated that, when metal concentrations exceed certain level (here, $\sum$THM > 337.4 μg g^{-1}), the carbon favored microbial activity declines (Jaiswal and Pandey 2019).

Nutrient supply stimulates microbial activity and decomposition of organic matter, and under appropriate temperature and water conditions, leads to high respiration and CO_2 emission (Liu et al. 2009). We found significant positive correlations between C availability and CO_2 emission at Asdr. However, at metal rich locations, this relationship implied up to certain levels only. As the concentration of metal increased, this relationship gone weaker. It seems that the microbial activities, and consequently the CO_2 release at LWI, are constrained by high concentration of toxic metals. Previous studies support these observations (Jaiswal and Pandey 2019). At Rmdr, the CO_2 emission was found to be low at drain mouth followed by an increasing trend indicating that metal stressors inhibit enzyme activities, and thereby , the emission of CO_2. At Asdr, the enzyme activities and emission of CO_2 showed a response almost synchronous to changes in the concentration of organic carbon. The C rich sites, characterized by faster rates of CO_2 emission, did show high activity of FDAase and β-D-glucosidase. The FDAase is used as a proxy of total microbial activity and organic matter turnover (Schnurere and Rosswall 1982), whereas the β-D-glucosidase is responsible for the hydrolysis of glycosidic bonds and used as marker of C acquisition (Sinsabaugh et al. 2009). The metal concentrations at Asdr did not appear high enough to induce inhibitory effects. On the contrary, the Rmdr Sites showed metal concentrations high enough to suppress enzyme activities, and consequently, the CO_2 emission. The carbon as a substrate stimulates EE activity while metal stressors can suppress it. However, under high concentrations of C and metals, the inhibition by the latter might counterbalance the substrate (carbon and nutrient)-driven stimulatory effects (Jaiswal and Pandey 2018). The dynamic fit model (Fig. 4) showed that total metal concentration above 337.4 μg g^{-1} induce adverse effects on CO_2 emission. In all the three subsets of studies, PCA separated metals opposite to CO_2 emission and microbial/enzyme activities. The NMDS yielded almost similar results. The Asdr Site showed low level of total heavy metal (ΣTHM < 337.4 μg g^{-1}), with microbial activities relatively higher and consequently the excess supply of C could assume importance triggering CO_2 emission. Previous studies have shown a marked decrease in C_{mic} and enzymes activities in metal polluted soils and sediments (Abaye et al. 2005; Li et al. 2009). We found significant positive relationships between qCO_2 and metal concentrations. Earlier studies show that C_{mic} declines and qCO_2 increases as metal concentration increases (Liu et al. 2012). Metal-associated changes in C-utilization have been considered as a microbial response to stressors and are used as an indicator of metal pollution (Brookes 1995). Overall, the patterns of CO_2 emission shown here demonstrate that the distribution of co-occurrence of metal and C-sources ultimately regulate the pattern of carbon sequestration in the Ganga River. Similar spatial trajectories can be expected for other human-impacted rivers suggesting the need of caution for regional C-budgeting and modeling.

Conclusions

The auto-and allochthonous–C input in human impacted large rivers is continuously increasing and these increases are often paralleled by almost similar increase in metal pollutants. Many lines of evidence presented here indicate that, although CO_2 emission in human-impacted large rivers is controlled by multiplicity of factors including chemical recalcitrance, high concentration of heavy metals suppresses the microbial-extracellular enzyme activities responsible for organic matter decomposition and consequently, the magnitude of CO_2 emission. Although we still have very less knowledge of how and to

what magnitude metal enrichment will effect organic matter decomposition and CO_2 release, our study clearly indicates that at source oriented locations, total metal concentration was sufficient to suppress microbial/enzyme activities vis-à-vis CO_2 release. We conclude that the overall impacts of heavy metal pollution on large rivers are probably much larger than what is generally predicted. When riverine-C sequestration is considered, a completely different scenario emerges: a transition towards metal pollution leads to increase C storage relative to loss as CO_2. This has implications for understanding C-cycling in human-impacted river sediments where metal pollution shields microbial degradation, and consequently, carbon and nutrient release. While this type of analysis is urgently needed from a climate change perspective, further studies need to include carbon-stabilizing effects for assessing ecosystem level impacts of heavy metal pollution for management and rejuvenation of large rivers.

Declarations

Ethics approval and consent to participate Not applicable.

Consent for publication Not applicable.

Competing interests The authors declare no competing interests.

Funding information This study was fully funded by National Academy of Science (India).

Availability of data and materials All data generated or analysed during this study are included in this published article.

Authors' contributions

K.V. contributed in data collection, validation, formal analysis, investigation, data curation, writing - original draft, funding acquisition.

J.P. contributed to designing of research idea review and editing of the original draft (preparation and creation of the paper), in the visualization process, formal analysis (analysing the study data) and supervision, acting as the corresponding author of this manuscript.

Acknowledgements The authors thank Coordinators of the Centre of Advanced Study in Botany and DST-FIST, Banaras Hindu University for facilities.

References

1. Abaye DA, Lawlor K, Hirsch PR, Brookes PC (2005) Changes in the microbial community of an arable soil caused
2. by long-term metal contamination. European J Soil Sci 56: 93–102
3. Adam G, Duncan H (2001) Development of a sensitive and rapid method for the measurement of total microbial activity using fluorescein diacetate (FDA) in a range of soils. Soil Biol Biochem 33:943–951
4. Aufdenkampe AK, Mayorga E, Raymond PA, Melack JM, Doney SC, Alin SR, Aalto RE, Yoo (2011) Riverine coupling of biogeochemical cycles between land, oceans, and atmosphere. Front Ecol Environ 9:53–60
5. Austin AT, Vivanco L (2006) Plant litter decomposition in a semi-arid ecosystem controlled by photodegradation. Nature 442:555–558
6. Bartoli G, Papa S, Sagnella E, Fioretto A (2012) Heavy metal content in sediments along the Calore river: relationships with physical–chemical characteristics. J Environ Manage 95:S9–S14
7. Battin TJ (1997) Assessment of fluorescein diacetate hydrolysis as a measure of total esterase activity in natural stream sediment biofilms. Sci Total Environ 198:51–60
8. Berggren M, del Giorgio PA (2015) Distinct patterns of microbial metabolism associated to riverine dissolved organic carbon of different source and quality. J Geophys Res Biogeo 120:989–999

9. Bernot MJ, Sobota DJ, Hall RO, Mulholland PJ, Dodds WK, Webster JR, Tank JL, Ashkenas LR, Cooper LW (2010) Inter-regional comparison of land-use effects on stream metabolism. Freshwater Biol 55:1874–1890
10. Boerjan W, Ralph J, Baucher M (2003) Lignin biosynthesis
11. Annu Rev Plant Biol 54: 519–546
12. Bose SK, Francis RC, Govender M, Bush T, Spark A (2009) Lignin content versus syringyl to guaiacyl ratio amongst poplars. Bioresour Technol 100:1628–1633
13. Boyero L, Pearson RG, Gessner MO, Barmuta LA, Ferreira V, Graça MA, West DC (2011) A global experiment suggests climate warming will not accelerate litter decomposition in streams but might reduce carbon sequestration. Ecol Lett 14:289–294
14. Brooke PC, Powlson DS, Jenkinson DS (1982) Measurement of microbial biomass phosphorus in soil. Soil boil biochem 14:319–329
15. Brookes PC (1995) The use of microbial parameters in monitoring soil pollution by heavy metals. Biol Fertil Soils 19:269–279
16. Butman D, Raymond PA (2011) significant efflux of carbon dioxide from streams and rivers in the United States. Nature Geosci 4:839
17. Catalán N, Marcé R, Kothawala DN, Tranvik LJ (2016) Organic carbon decomposition rates controlled by water retention time across inland waters. Nature Geosci 9:501–504
18. Ciavatta C, Govi M, Antisari LV, Sequi P (1991) Determination of organic carbon in aqueous extracts of soils and fertilizers. Commun Soil Sci Plant Anal 22:795–807
19. Cole JJ, Caraco NF (2001) Carbon in catchments: connecting terrestrial carbon losses with aquatic metabolism. Mar Freshwater Res 52:101–110
20. Cole JJ, Prairie YT, Caraco NF, McDowell WH, Tranvik LJ, Striegl RG, Duarte CM, Kortelainen P, Downing JA, Middelburg JJ, Melack J (2007) Plumbing the global carbon cycle: integrating inland waters into the terrestrial carbon budget. Ecosystems 10:172–185
21. Dai XY, Ping CL, Michaelson GJ (2002) Characterizing soil organic matter in Arctic tundra soils by different analytical approaches. Organic Geochem 33:407–419
22. Dick RP (2020) Methods of soil enzymology John Wiley & Sons Vol:26
23. Dobler R, Saner M, Bachofen R (2000) Population changes of soil microbial communities induceby hydrocarbon and heavy metal contamination. Bioremediat J 4:41–56
24. Eivazi F, Tabatabai MA (1988) Glucosidases and galactosidases in soils. Soil Biol Biochem 20:601–606
25. Farkas A, Erratico C, Vigano L (2007) Assessment of the environmental significance of heavy metal pollution in surficial sediments of the River Po. Chemosphere 68:761–768
26. Ford TE (2000) Response of marine microbial communities to anthropogenic stress. J Aquatic Ecosys Stress Recov 7:75–89
27. Foulquier A, Artigas J, Pesce S, Datry T (2015) Drying responses of microbial litter decomposition and associated fungal and bacterial communities are not affected by emersion frequency. Freshwater Sci 34:1233–1244
28. Freeman C, Ostle N, Kang H (2001) An enzymic 'latch' on a global carbon store - a shortage of oxygen locks up carbon in peatlands by restraining a single enzyme. Nature 409:149
29. Freeman C, Ostle NJ, Fenner N, Kang H (2004) A regulatory role for phenol oxidase during decomposition in peatlands. Soil Biol Biochem 36:1663–1667
30. Gessner MO, Swan CM, Dang CK, McKie BG, Bardgett RD, Wall DH, Hättenschwiler S (2010) Diversity meets decomposition. Trends Ecol Evol 25:372–380
31. Guérin F, Abril G, Richard S, Burban B, Reynouard C, Seyler P, Delmas R (2006) Methane and carbon dioxide emissions from tropical reservoirs: significance of downstream rivers. Geophys Res Lett 33:(21)

32. Houghton R, Lawrence K, Hackler J, Brown (2001) The spatial distribution of forest biomass in the Brazilian Amazon: A comparison of estimates. Glob Change Biol 7:731–746
33. Hu M, Ren H, Ren P, Li J, Wilson BJ, Tong C (2017) Response of gaseous carbon emissions to low-level salinity increase in tidal marsh ecosystem of the Min River estuary, southeastern China. J Environ Sci 52:210–222
34. Jaiswal D, Pandey J (2018) Impact of heavy metal on activity of some microbial enzymes in the riverbed sediments: Ecotoxicological implications in the Ganga River (India). Ecotoxic Environ Saf 150:104–115
35. Jaiswal D, Pandey J (2019) Carbon dioxide emission coupled extracellular enzyme activity at land-water interface predict C-eutrophication and heavy metal contamination in Ganga River, India. Ecol Indic 99:349–364
36. Jenkinson DS, Powlson DS (1976) The effects of biocidal treatments on metabolism in soil—V: A method for measuring soil biomass. Soil Bio Biochem 8:209–213
37. Johnson D, Leake JR, Lee JA, Campbell CD (1998) Changes in soil microbial biomass and microbial activities in response to 7 years simulated pollutant nitrogen. Environ Pollut 103:239–250
38. Kandeler E, Stemmer M, Klimanek EM (1999) Response of soil microbial biomass, urease and xylanase within particle size fractions to long-term soil management. Soil Bio Biochem 31:261–273
39. KS K, XIE Z, HUANC C (1998) Relative toxicity of lead chloride and lead acetate to microbial biomass in red soil. Chinese J Appl Environ Bio 02
40. Ladd JN, Butler JHA (1972) Short-term assays of soil proteolytic enzyme activities using proteins and dipeptide derivatives as substrates. Soil Bio Biochem 4:19–30
41. Lau DCP, Leung KMY, Dudgeon D (2009) What does stable isotope analysis reveal about trophic relationships and the relative importance of allochthonous and autochthonous resources in tropical streams? A synthetic study from Hong Kong. Freshwater Biol 54:127–141
42. Le Quéré C, Peters GP, Andres RJ, Andrew RM, Boden TA, Ciais P, Friedlingstein P, Houghton RA, Marland G, Moriarty R, Sitch S (2014) Global carbon budget 2013. Earth Sys Sci Data 6:235–263
43. Lee SS, Shin KJ, Kim WY, Ha JK, Han IK (1999) The rumen ecosystem: As a fountain source of nobel enzymes-Review. Asian-Australasian J Ani Sci 12:988–1001
44. Li YT, Rouland C, Benedetti M, Li FB, Pando A, Lavelle P, Dai J (2009) Microbial biomass, enzyme and mineralization activity in relation to soil organic C, N and P turnover influenced by acid metal stress. Soil Biol Biochem 41:969–977
45. Liu W, Zhang ZHE, Wan S (2009) Predominant role of water in regulating soil and microbial respiration and their responses to climate change in a semiarid grassland. Glob Change Biol 15:184–195
46. Liu Y, Zhou T, Crowley D, Li L, Liu D, Zheng J, Yu X, Pan G, Hussain Q, Zhang X, Zheng J (2012) Decline in top soil microbial quotient, fungal abundance and C utilization efficiency of rice paddies under heavy metal pollution across South China. PLoS One 7:38858
47. Lorenzen C, Jeffrey J (1980) Determination of chlorophyll in sea water. Unesco Techn Papers Marine Sci 35
48. Malhi Y, Roberts JT, Betts RA, Killeen TJ, Li W, Nobre CA (2008) Climate change, deforestation, and the fate of the Amazon. Science 319:169–172
49. Mariscal-Sancho I, Santano J, Mendiola M, Peregrina F, Espejo R (2010) Carbon dioxide emission rates and β-glucosidase activity in Mediterranean Ultisols under different soil management. Soil Sci 175:453–460
50. Mayorga E, Aufdenkampe AK, Masiello CA, Krusche AV, Hedges JI, Quay PD, Richey JE, Brown TA (2005) Young organic matter as a source of carbon dioxide outgassing from Amazonian rivers. Nature 436:538–541
51. McLatchey GP, Reddy KR (1998) Regulation of organic matter decomposition and nutrient release in a wetland soil. American Society Agron, Crop Sci Society America and Soil Sci Society America. 27:1268–1274
52. Murphy JAMES, Riley JP (1962) A modified single solution method for the determination of phosphate in natural waters. Anal Chim Acta 27:31–36
53. Pandey J, Pandey U, Singh AV (2014) Impact of changing atmospheric deposition chemistry on carbon and nutrient loading to Ganga River: integrating land–atmosphere–water components to uncover cross-domain carbon linkages.

Biogeochemistry 119:179–198

54. Pandey J, Yadav A (2017) Alternative alert system for Ganga river eutrophication using alkaline phosphatase as a level determinant. Ecol Indi 82:327–343
55. Park JH, Nayna OK, Begum MS, Chea E, Hartmann J, Keil RG, Kumar S, Lu X, Ran L, Richey JE, Sarma VV (2018) Reviews and syntheses: Anthropogenic perturbations to carbon fluxes in Asian river systems–concepts, emerging trends, and research challenges. Biogeosciences 15:3049–3069
56. Raymond PA, Hartmann J, Lauerwald R, Sobek S, McDonald C, Hoover M, Butman D, Striegl R, Mayorga E, Humborg C, Kortelainen P (2013) Global carbon dioxide emissions from inland waters. Nature 503:355–360
57. Richey JE, Melack JM, Aufdenkampe AK, Ballester VM, Hess LL (2002) Outgassing from Amazonian rivers and wetlands as a large tropical source of atmospheric CO_2. Nature 416:617
58. Romaní AM, Guasch H, Muñoz I, Ruana J, Vilalta E, Schwartz T, Emtiazi F, Sabater S (2004) Biofilm structure and function and possible implications for riverine DOC dynamics. Microbiol Ecol 47:316–326
59. Rosemond AD, Benstead JP, Bumpers PM, Gulis V, Kominoski JS, Manning DW, Suberkropp K, Wallace JB (2015) Experimental nutrient additions accelerate terrestrial carbon loss from stream ecosystems. Science 347:1142–1145
60. Rubio B, Nombela MA, Vilas F (2000) Geochemistry of major and trace elements in sediments of the Ria de Vigo (NW Spain): an assessment of metal pollution. Marine Pollut Bullet 40:968–980
61. Sayler GS, Puziss M, Silver M (1979) Alkaline phosphatase assay for freshwater sediments: application to perturbed sediment systems. Appl Environ Microbiol 38:922–927
62. Schimel JP, Weintraub MN (2003) The implications of exoenzyme activity on microbial carbon and nitrogen limitation in soil: a theoretical model. Soil Biol Biochem 35:549–563
63. Schnürer J, Rosswall T (1982) Fluorescein diacetate hydrolysis as a measure of total microbial activity in soil and litter. Appl Environ Microbiol 43:1256–1261
64. Shen SM, Pruden G, Jenkinson DS (1984) Mineralization and immobilization of nitrogen in fumigated soil and the measurement of microbial biomass nitrogen. Soil Biol Biochem 16:437–444
65. Siddiqui E, Pandey J, Pandey U, Mishra V, Singh AV (2020) Integrating atmospheric deposition-driven nutrients (N and P), microbial and biogeochemical processes in the watershed with carbon and nutrient export to the Ganga River. Biogeochemistry 147:149–178
66. Singh R, Pandey J (2018) Non-point source-driven carbon and nutrient loading to Ganga River (India). Chem Ecol 35:344–360
67. Sinsabaugh RL (2010) Phenol oxidase, peroxidase and organic matter dynamics of soil. Soil Biol Biochem 42:391–404
68. Sinsabaugh RL, Findlay S (1995) Microbial production, enzyme activity and carbon turnover in surface sediments of the Hudson River Estuary. Microbial Ecol 30:127–141
69. Sinsabaugh RL, Hill BH, Shah JJF (2009) Ecoenzymatic stoichiometry of microbial organic nutrient acquisition in soil and sediment. Nature 462:795–798
70. Sinsabaugh RL, Lauber CL, Weintraub MN, Ahmed B, Allison SD, Crenshaw C, Contosta AR, Cusack D, Frey S, Gallo ME, Gartner TB (2008) Stoichiometry of soil enzyme activity at global scale. Ecol lett 11:1252–1264
71. Smith VH, Schindler DW (2009) Eutrophication science: where do we go from here? Trends Ecol Evolut 24:201–207
72. Stemmer M, Gerzabek MH, Kandeler E (1998) Invertase and xylanase activity of bulk soil and particle-size fractions during maize straw decomposition. Soil Biol Biochem 31:9–18
73. Tabatabai MA, Bremner JM (1969) Use of p-nitrophenyl phosphate for assay of soil phosphatase activity. Soil Biol Biochem 1:301–307
74. Taylor PG, Townsend AR (2010) Stoichiometric control of organic carbon–nitrate relationships from soils to the sea. Nature 464:1178–1181

75. Teodoru CR, Nyoni FC, Borges AV, Darchambeau F, Nyambe I, Bouillon S (2015) Dynamics of greenhouse gases (CO_2, CH_4, N_2O) along the Zambezi River and major tributaries, and their importance in the riverine carbon budget. Biogeosciences 12:2431–2453
76. Tezuka Y (1990) Bacterial regeneration of ammonium and phosphate as affected by the carbon: nitrogen: phosphorus ratio of organic substrates. Microbial Ecol 19:227–238
77. Van den Meersche K, Van Rijswijk P, Soetaert K, Middelburg JJ (2009) Autochthonous and allochthonous contributions to mesozooplankton diet in a tidal river and estuary: integrating carbon isotope and fatty acid constraints. Limnol Oceanogr 54:62–74
78. Vannote RL, Minshall GW, Cummins KW, Sedell JR, Cushing CE (1980) The river continuum concept. Can J Fish Aquat Sci 37:130–137
79. Verma K, Pandey J (2019) Heavy metal accumulation in surface sediments of the Ganga River (India): speciation, fractionation, toxicity, and risk assessment. Environ Monit Assess 191:414
80. Ward ND, Keil RG, Medeiros PM, Brito DC, Cunha AC, Dittmar T, Yager PL, Krusche AV, Richey JE (2013) Degradation of terrestrially derived macromolecules in the Amazon River. Nature Geosci 6:530–533
81. Wardle DA, Yeates GW, Watson RN, Nicholson KS (1993) Response of soil microbial biomass and plant litter decomposition in maize and asparagus cropping systems. Soil Biol Biochem 25:857–868
82. Yadav A, Pandey J (2017) Contribution of point sources and non-point sources to nutrient and carbon loads and their influence on the trophic status of the Ganga River at Varanasi, India. Environ Monit Assess 189:1–19
83. Yan J, Pan G, Li L, Quan G, Ding C, Luo A (2010) Adsorption, immobilization, and activity of β-glucosidase on different soil colloids. J Colloid Interface Sci 348:565–570

Tables

Table 1 Biogeochemical characteristics of sediment at land-water interface (LWI) at different sampling sites of Ganga River during low flow period

Sites	Cond (µS cm^{-1})	WSOC (mg kg^{-1})	TOC (%)	TN (%)	C:N ratio	C_{mic} (µg g^{-1})	N_{mic} (µg g^{-1})	P_{mic} (µg g^{-1})	SRP (mg g^{-1})	Chl **a** (µg g^{-1})	Coarse sand (%)	Fine sand (%)	Silt (%)	Clay (%)
Dvpg	200	450	1.56	0.1	15.6	280	28	16.8	0.5	8	54	23	14	9
Htwa	280	850	3.6	0.3	12	600	50	28	1.2	12	22	25	33	20
Sngm	380	980	4.5	0.45	10	750	78	45	2	16	12	18	25	45
Stmh	270	780	2.5	0.2	12.5	500	45	25	1	13	25	25	30	20
Adpr	260	710	2.2	0.15	14.6	432	38	20	0.8	10	22	42	23	13
Rmna	300	970	4	0.35	11.4	700	70	32	1.5	14	18	22	25	35
Rjht	400	1100	9	0.49	18.1	350	40	20	2.8	3	10	12	25	53

Cond: conductivity; WSOC: water soluble organic carbon; TOC: total organic carbon; C_{mic}: microbial carbon; N_{mic}: microbial nitrogen; P_{mic}: microbial phosphorus

Table 2 Biogeochemical characteristics of sediment at land-water interface (LWI) at different sampling sites during low flow period of Assi drain (Asdr). The zero represents drain mouth whereas – sign shows upstream sites.

Sites (m)	Cond ($\mu S\ cm^{-1}$)	WSOC (mg kg^{-1})	TOC (%)	TN (%)	C:N ratio	C_{mic} ($\mu g\ g^{-1}$)	N_{mic} ($\mu g\ g^{-1}$)	P_{mic} ($\mu g\ g^{-1}$)	SRP (mg g^{-1})	Chl **a** ($\mu g\ g^{-1}$)	Coarse sand (%)	Fine sand (%)	Silt (%)	Clay (%)
-1500	342	650	2.4	0.08	30	340	35	18	0.8	18	15	34	27	24
-1400	344	680	2.6	0.09	28	432	39	22	1.2	21	14.8	33	26.2	25
-1300	348	734	2.8	0.10	28	490	46.3	25	1.54	23.4	14	31	25.7	27
-1200	352	792	3.2	0.12	26.6	532	49.7	29	1.87	28.5	13.7	30.4	25.4	28.4
-1100	355	845	3.7	0.13	24.6	587	53.5	35.2	2.3	32.5	13.5	29.6	25.2	30.3
-1000	358	923	3.9	0.13	26	643	59.2	39.6	2.6	38.5	13.2	27.5	25	32.4
-900	360	956	4.5	0.18	25	752	64.3	43.2	2.9	42.3	13	25	24.7	35
-800	364	1013	4.8	0.2	24	821	68.4	48.6	3.3	47.6	12.4	23.4	24.5	38
-700	368	1056	5.2	0.22	23.6	875	75.3	50.2	3.5	48.2	12.1	22.1	24.3	42
-600	372	1105	5.6	0.23	24.3	934	79.7	52.4	3.8	48.7	11.6	20	24	46
-500	374	1154	6.2	0.25	24.8	976	88.5	53.7	4.1	49.5	11	18	23.67	47
-400	376	1198	6.4	0.26	24.6	1004	92.5	54.2	4.5	50.2	10.76	16.3	23.43	48
-300	377	1205	6.5	0.27	24.	1065	96.4	56.4	4.8	51.3	10	14.3	23.3	50
-200	378	1217	7	0.3	23.3	1078	97.5	56.8	5.2	52	9.67	13.2	22.8	52
-100	379	1234	8	0.34	23.5	1083	103	57.2	5.5	53	9.2	12.8	22.5	55
0	380	1250	9	0.4	22.5	1100	110	58	5.6	55	8	12	22	58
100	376	1200	8.8	0.38	23.1	1007	108	53	5.1	53	8.5	16	20	55
200	375	1178	8.5	0.36	23.6	895	103	48	4.6	48	8.9	18	19	54
300	372	1132	8.2	0.32	25.6	823	98	42	4	44	9.1	22	17	52
400	370	1045	8	0.3	26.6	754	93	38	3.6	41	9.3	25	16	48
500	369	1031	7.8	0.29	26.8	712	86	35	3.2	38	9.8	29	15	42
600	365	995	7.64	0.27	28.2	698	82	30	3	36	10.2	32	14.8	38
700	364	973	7.6	0.25	30.4	674	79	28	2.8	33	10.8	35	14	26
800	363	967	6.4	0.24	26.6	645	73	27.5	2.6	31	11.4	39	13.6	20
900	362	932	5.9	0.23	29.5	621	67	27.3	2.3	28	11.6	42	13.4	19
1000	362	856	5.4	0.21	27	607	64	26.8	2.1	25	11.7	45	13	17
1100	361	831	4.8	0.19	25.2	589	60	26.3	1.7	24	11.8	47	12	16
1200	358	803	4.5	0.17	26.4	583	57	26.2	1.4	22	11.9	48	11.5	15.
1300	357	793	4.2	0.16	26.2	582	52	25.8	1.3	20.5	12.2	49	11.3	15
1400	354	784	4.2	0.15	28	581	50	25.4	1.2	20.2	12.4	49.6	11.2	15
1500	350	780	4.2	0.14	30	580	50	25.3	1.2	20	12.5	50	11.2	15

Cond: conductivity; WSOC: water soluble organic carbon; TOC: total organic carbon; C_{mic}: microbial carbon; N_{mic}: microbial nitrogen; P_{mic}: microbial phosphorus

Table 3 Biogeochemical characteristics of sediment at land-water interface (LWI) at different sampling sites during low flow period of Ramnagar drain (Rmdr). The zero represents drain mouth whereas – sign shows upstream sites.

Cond: conductivity; WSOC: water soluble organic carbon; TOC: total organic carbon; C_{mic}: microbial carbon; N_{mic}: microbial nitrogen; P_{mic}: microbial phosphorus

Table 4 Loading of the sediment quality variables studied at the main stem river, Assi drain (Asdr) and Ramnagar drain (Rmdr) on significant principal components (Varifactor; VF)

Sites	Cond (µS cm^{-1})	WSOC (mg kg^{-1})	TOC (%)	TN (%)	C:N ratio	C_{mic} (µg g^{-1})	N_{mic} (µg g^{-1})	P_{mic} (µg g^{-1})	SRP (mg g^{-1})	Chl **a** (µg g^{-1})	Coarse sand (%)	Fine sand (%)	Silt (%)	Clay (%)
-1500	382	540	2	0.18	14	648	56	43	1	43	28	30	22	20
-1400	378	564	2.4	0.21	15	621	53	41.2	1.03	32	25	29	25	21
-1300	373	648	2.6	0.24	15.3	598	51	37.5	1.08	27	24	27	26	23
-1200	370	683	2.8	0.26	15.6	576	48	31.3	1.12	21	23	25	28	24
-1100	368	723	3.2	0.27	16	523	45	27.5	1.32	18	22	24	28.5	25.5
-1000	365	756	3.3	0.29	16.6	489	41.3	25.3	1.58	16	21	23.6	29	26.4
-900	364	798	3.6	0.3	17	457	39.6	22.6	1.83	14.3	20.2	23	29.8	27
-800	362	835	3.98	0.32	17.4	432	38.5	18.4	1.92	12	19	22.8	31	27.2
-700	361	868	4.3	0.33	17.8	354	36.3	16.8	2.1	10.2	18.2	22.3	31.5	28
-600	360	934	4.7	0.35	18	310	32.4	14.3	2.23	10	16.2	22	31.8	30
-500	359	986	4.9	0.37	18.5	286	30.4	12.6	2.45	9.8	15.8	21.7	32	30.5
-400	358	992	5.2	0.38	18.9	254	28.5	12.4	2.67	9.5	14.1	21.6	32.2	32.1
-300	354	997	5.4	0.39	19.3	224	24.5	12.0	2.83	9.3	13.5	21	32.3	33.2
-200	353	998	5.7	0.39	19.6	213	22.3	11.7	2.95	9	12.7	20.8	32.8	33.7
-100	353	999	5.8	0.39	20	206	21.3	11.4	3.2	8.5	12.3	20.3	33	34.4
0	352	1006	6	0.5	23.2	200	20	10	3.5	8	12	20	33	35
100	354	980	5.6	0.38	21.6	253	20.4	11.2	3.23	9.3	12.4	21.3	31.8	34.5
200	356	945	5.3	0.36	21.3	268	20.7	13.5	3.15	11.56	12.8	22.6	31.4	33.2
300	357	912	5.2	0.35	21	312	30.3	16	3.06	13.2	13.1	23.7	31.2	32
400	358	893	5	0.33	20	358	30.7	18	2.86	15.8	13.8	24	31	31.2
500	360	864	4.8	0.32	19.6	397	30.9	22	2.74	17.4	14.6	25	30	30.4
600	361	804	4.5	0.3	17.6	414	40.2	25	2.53	20.3	14.7	25.2	30.1	30
700	363	789	4.1	0.29	17.2	456	40.4	28	2.39	22.6	15	25.6	30	29.4
800	364	754	3.9	0.28	16	480	40.5	30	2.23	24.8	16.2	25.8	29.5	28.5
900	365	732	3.5	0.28	12.3	502	40.6	32	2.12	26.5	17	26	29	28
1000	367	720	3.2	0.28	11.4	578	40.8	34	2.07	27.9	18.4	27.3	28.3	26
1100	368	712	3	0.28	10.7	582	40.8	35.7	2.03	28.3	21.2	29.6	25	24.2
1200	369	708	2.8	0.28	10	588	40.9	37	2	29.8	22.3	30.4	24.3	23
1300	371	706	2.6	0.28	9.2	592	40.9	38	1.52	31.4	23.2	31.2	25.3	20.3
1400	372	703	2.5	0.27	9.2	596	50	39	1.3	31.8	25	32	23	20
1500	372	700	2.5	0.27	9.2	600	50	40	1	32	25.2	32.1	23	19.7

	Main stem			Asdr			Rmdr	
	VF 1	VF 2	VF3	VF 1	VF 2	VF3	VF 1	VF 2
Zn	**0.78**	-0.24	-0.08	0.54	**0.89**	-0.01	**0.88**	-0.21
Cr	**0.82**	-0.21	-0.02	-0.43	**0.85**	-0.03	**0.82**	-0.16
Cu	**0.85**	-0.15	-0.01	0.52	**0.74**	-0.02	**0.84**	0.12
Pb	**0.80**	0.19	-0.03	-0.42	**0.83**	-0.03	**0.73**	0.14
Cd	**0.74**	0.24	-0.04	-0.34	**0.85**	-0.05	**0.81**	-0.18
Ni	**0.72**	0.16	-0.05	0.35	**0.74**	-0.02	**0.86**	-0.21
qCO_2	**0.88**	0.14	-0.02	0.21	**0.84**	-0.04	**0.82**	0.19
Cond	**0.68**	-0.35	-0.04	**0.76**	-0.23	-0.02	**0.61**	-0.12
SRP	**0.72**	-0.23	-0.06	**0.78**	-0.22	-0.01	**0.68**	-0.18
TOC	**0.86**	-0.23	-0.02	**0.82**	**-**0.12	-0.02	**0.83**	0.10
TN	**0.82**	-0.26	-0.01	**0.80**	-0.13	-0.01	**0.82**	0.08
C:N ratio	-0.52	**0.62**	-0.03	**0.86**	-0.22	-0.02	**0.86**	0.12
WSOC	**0.84**	-0.24	-0.04	**0.83**	-0.18	-0.06	**0.78**	0.14
CO_2 emission	0.12	**0.89**	-0.02	**0.78**	-0.34	-0.04	-0.23	**0.76**
SIR	-0.04	**0.75**	-0.01	**0.88**	0.21	-0.05	-0.26	**0.73**
β-D-glucosidase	-0.22	**0.88**	-0.02	**0.81**	0.21	-0.06	-0.24	**0.85**
FDAase	-0.23	**0.83**	-0.01	**0.89**	-0.32	-0.04	-0.21	**0.83**
Protease	-0.15	**0.85**	-0.04	**0.82**	-0.20	-0.08	-0.16	**0.83**
Phenol oxidase	-0.18	0.27	**0.84**	0.21	-0.08	**0.84**	-0.21	**0.84**
AP	-0.12	0.23	**0.72**	0.23	-0.05	**0.82**	-0.18	**0.80**
C_{mic}	0.32	**0.80**	0.02	**0.83**	-0.34	0.02	0.18	**0.82**
N_{mic}	-0.12	**0.84**	0.03	**0.86**	-0.18	0.03	0.18	**0.83**
P_{mic}	-0.22	**0.80**	0.04	**0.83**	-0.17	0.04	0.12	**0.80**
Chl **a**	-0.23	**0.79**	0.03	**0.82**	-0.20	0.05	0.15	**0.81**
Coarse sand	**0.62**	0.23	0.17	**0.65**	0.55	0.01	**0.67**	0.20
Fine sand	**0.68**	0.14	0.23	**0.78**	0.32	0.03	**0.65**	0.22
Silt	**0.72**	-0.22	0.16	**0.82**	-0.21	0.02	0.18	**0.75**
Clay	**0.80**	-0.16	0.13	**0.85**	-0.20	0.02	0.03	**0.93**
% of Variance	62.12	20.02	9.95	66.12	22.21	8.9	67.13	27.04
% Cumulative	62.12	82.14	92.09	66.12	22.21	97.23	67.13	94.17

qCO_2: microbial metabolic quotient; Cond: conductivity; SRP: subustrate reactive phosphorus; TOC: total organic carbon; TN: total nitrogen; WSOC:water soluble organic carbon; SIR: substrate induced respiration; AP: alkaline phosphatase; C_{mic}:microbial carbon; N_{mic}: microbial nitrogen; P_{mic}: microbial phosphorus; C_{mic}: microbial biomass C

Figures

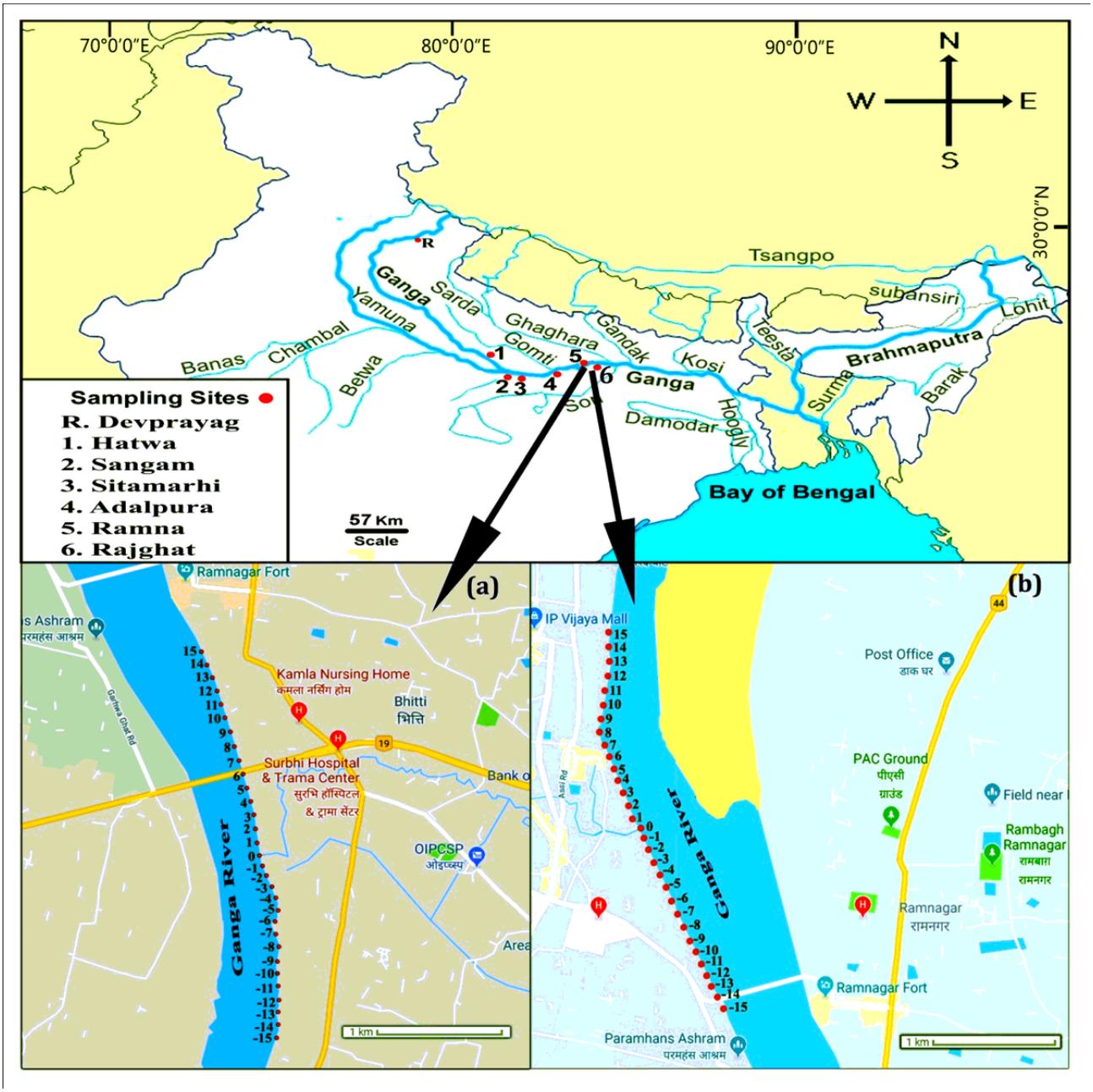

Figure 1

Map of the area showing study locations up- and down-stream of two point sources (a) Ramnagar drain and (b) Assi drain. Zero represents mouth of the outlet and – sign represents upstream locations to drain-mouth

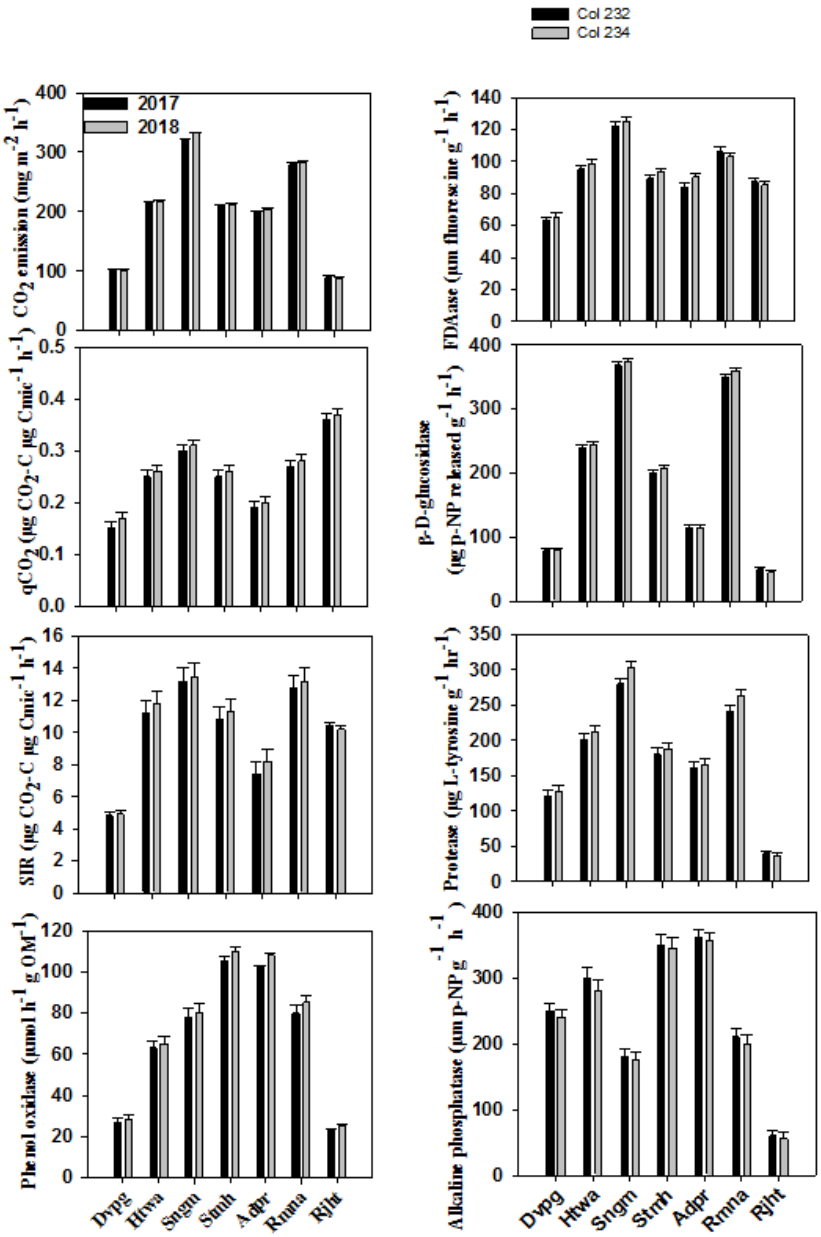

Figure 2

CO2 emission and regulatory variables at land-water interface of the main stem of the Ganga River. Values are mean (n=24) ± SD

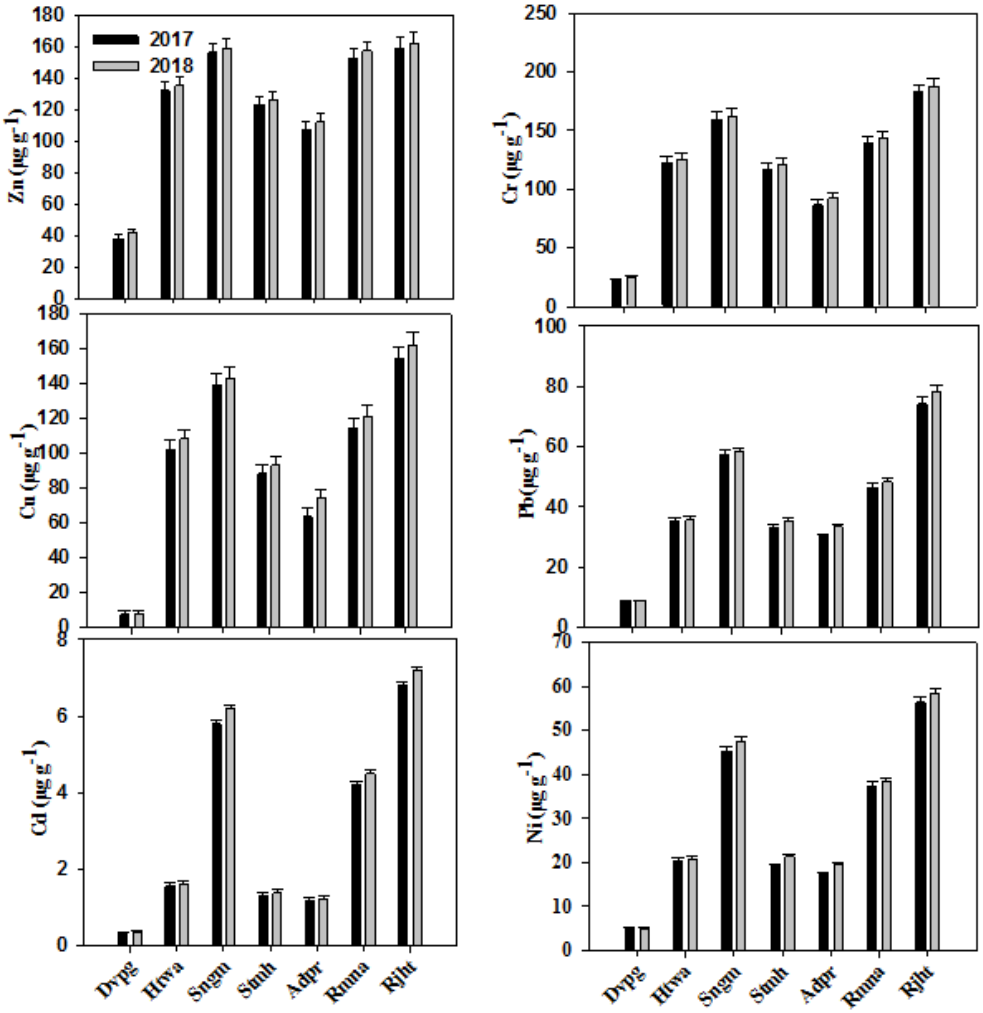

Figure 3

Heavy metal concentration at land-water interface of the main stem of the Ganga River. Values are mean (n= 24) ± SD

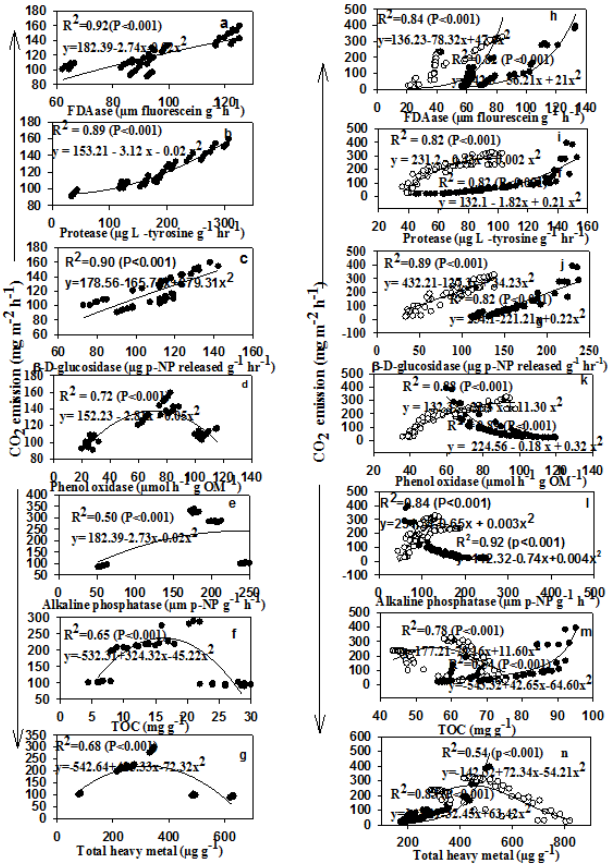

Figure 4

The dynamic fit model for CO2 emission showing relationship with regulatory variables at land-water interface of the main-stem (a to g) and two point sources (h to n) of the Ganga River

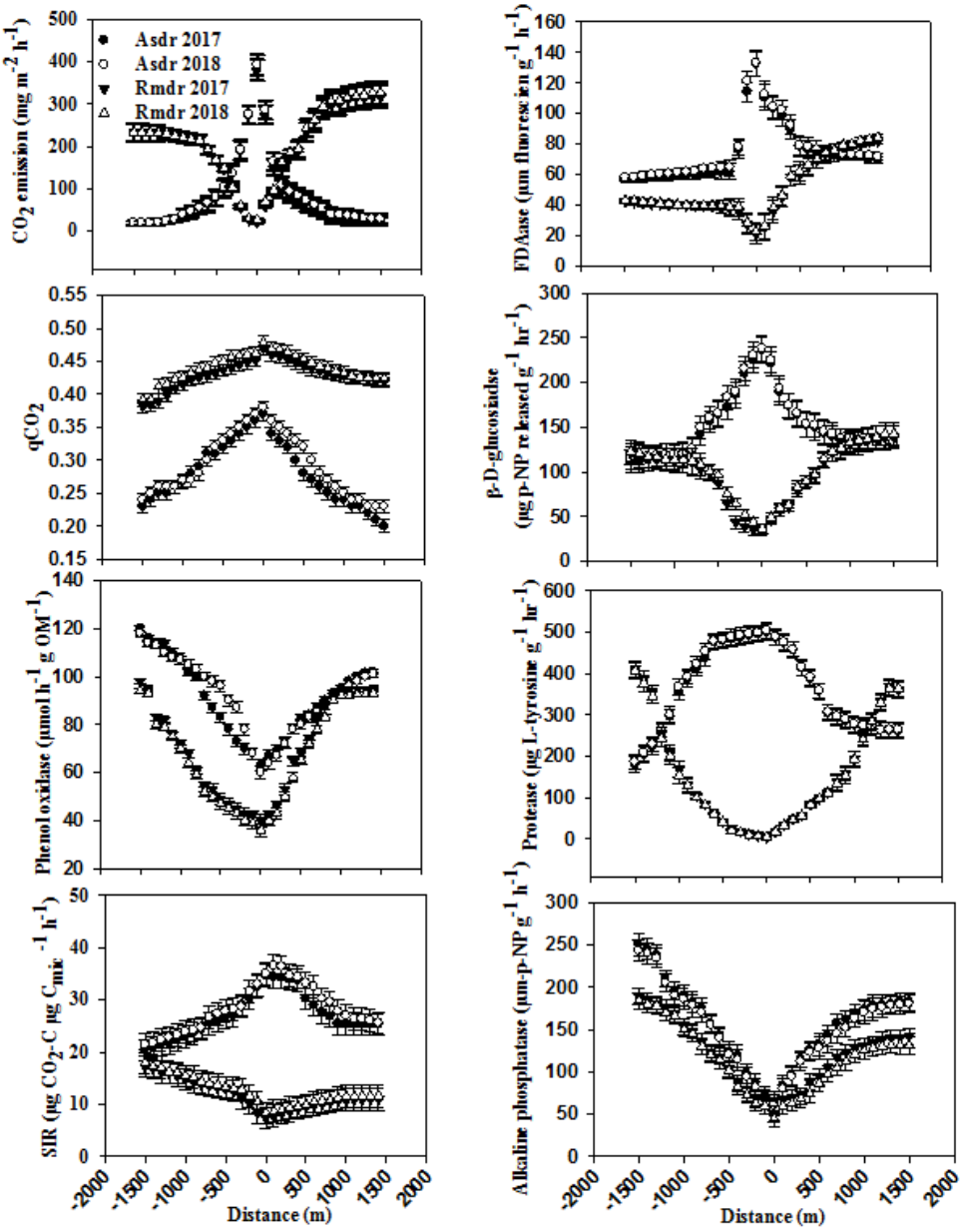

Figure 5

Point source up-and downstream trends in CO2 emission and regulatory variables at land-water interface of the Ganga River. Asdr: Assi drain; Rmdr: Ramnagar drain. The zero represents drain mouth whereas – sign shows upstream influences

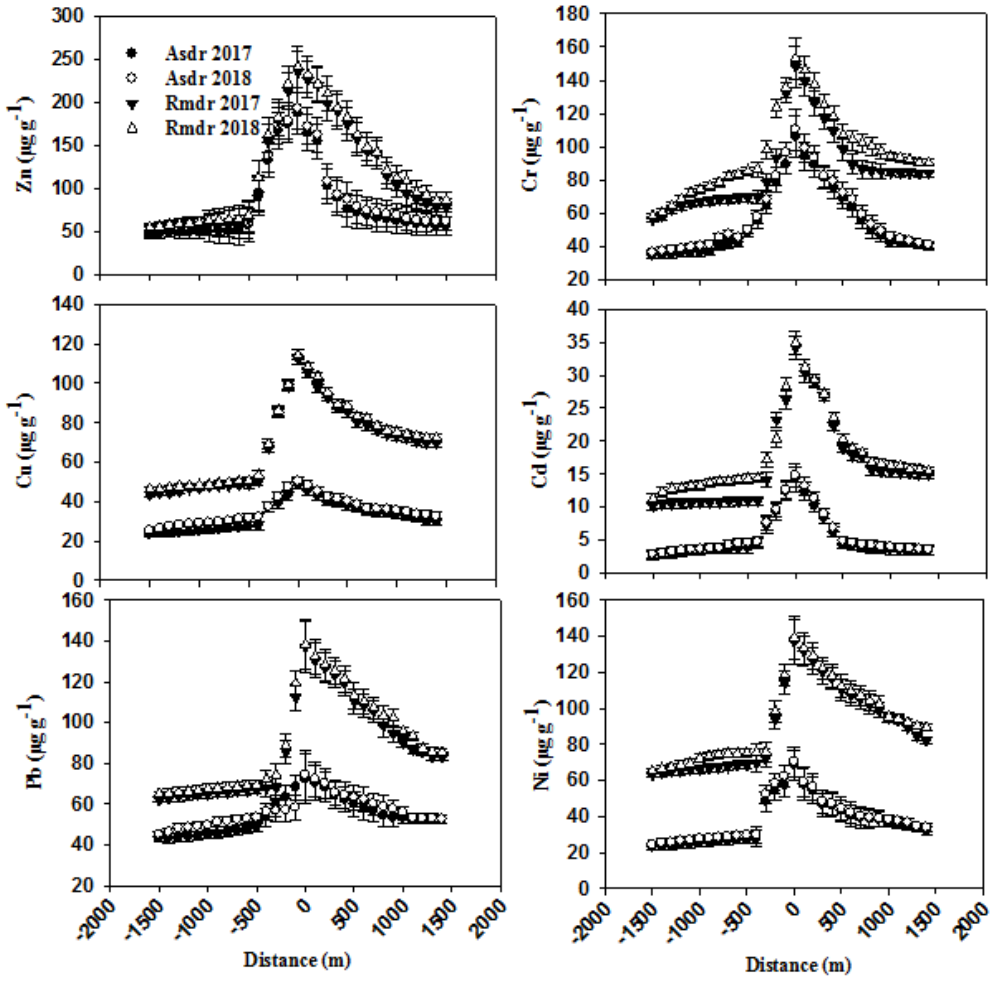

Figure 6

Point source up- and downstream trends in the concentration of heavy metals at land-water interface of the Ganga River. Asdr: Assi drain; Rmdr: Ramnagar drain. The zero represents drain mouth whereas – sign shows upstream influences

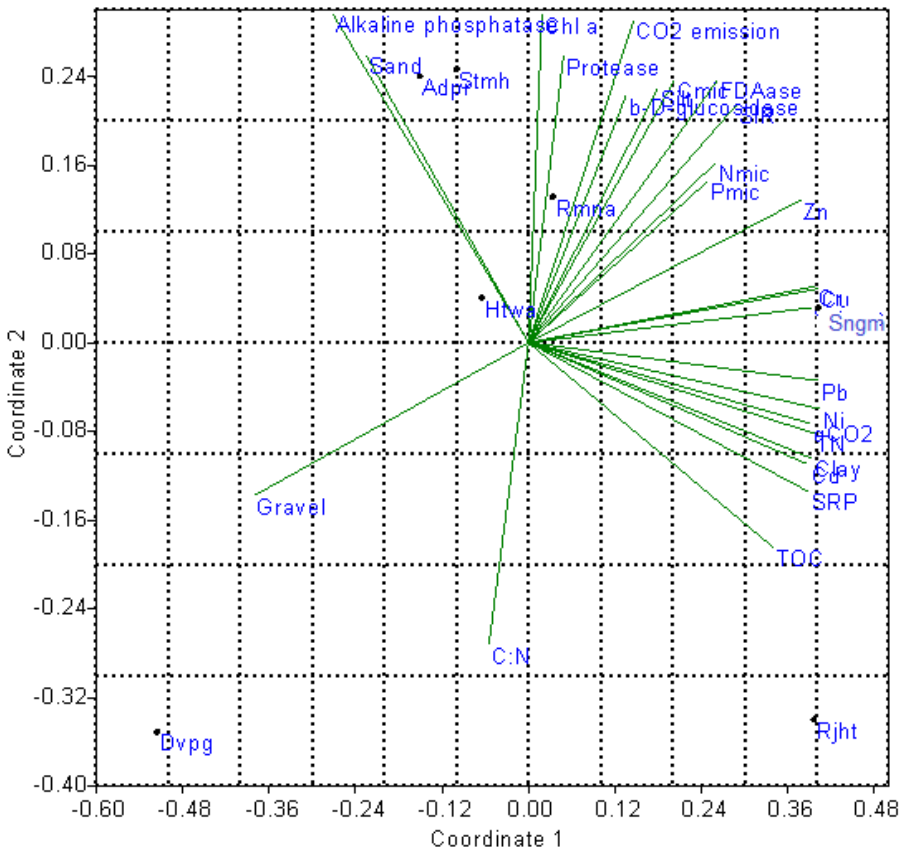

Figure 7

Non-metric multidimensional scaling (NMDS) segregating sites and study variables along main stem of Ganga River

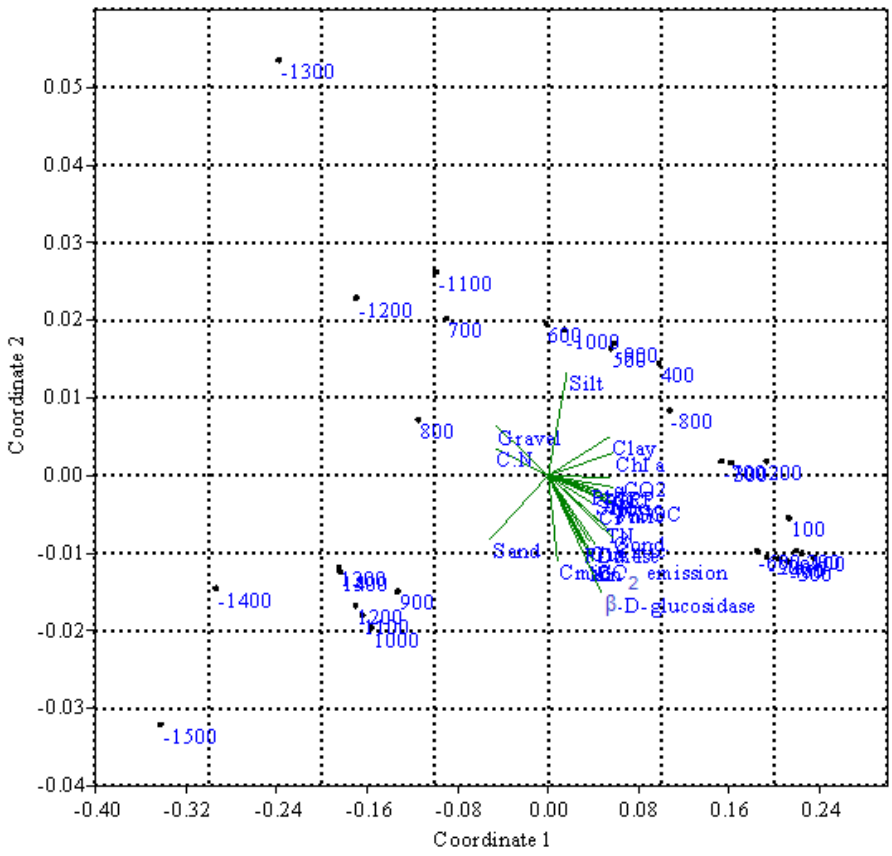

Figure 8

Non-metric multidimensional scaling (NMDS) segregating sites and study variables along upstream and downstream of Assi drain (Asdr)

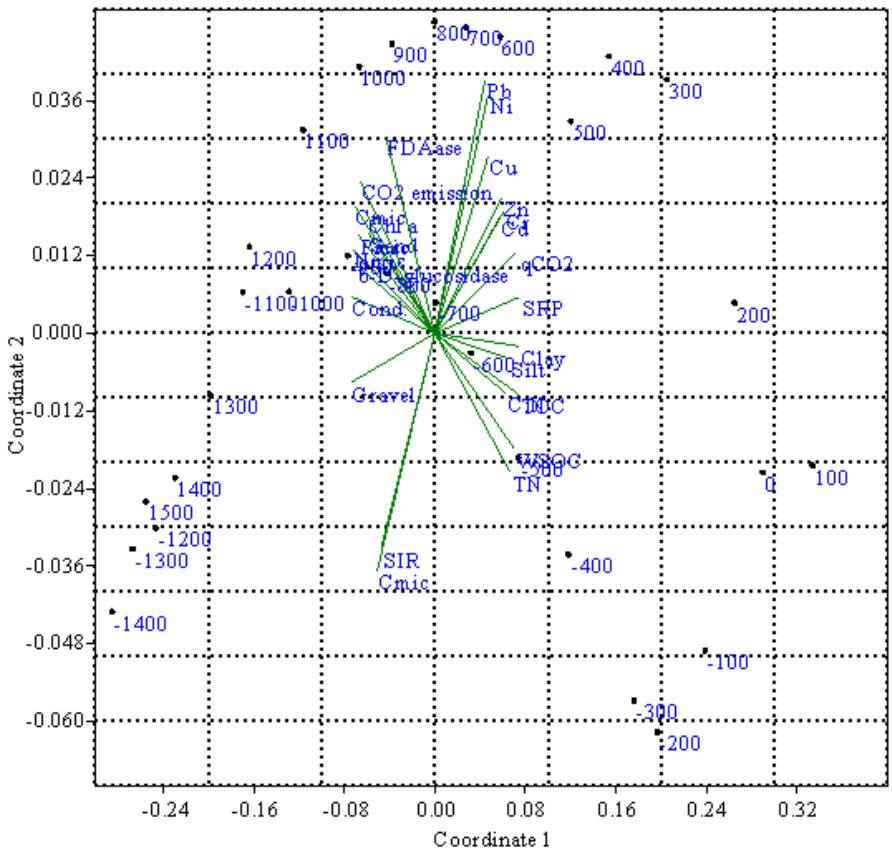

Figure 9

Non-metric multidimensional scaling (NMDS) segregating sites and study variables along upstream and downstream of Ramnagar drain (Rmdr)